



Universiteit  
Leiden  
The Netherlands

## Particle tracing based on 4D Flow Magnetic Resonance Imaging: a systematic review into methods, applications, and current developments

Roos, P.R.; Rijnberg, F.M.; Westenberg, J.J.M.; Lamb, H.J.

### Citation

Roos, P. R., Rijnberg, F. M., Westenberg, J. J. M., & Lamb, H. J. (2022). Particle tracing based on 4D Flow Magnetic Resonance Imaging: a systematic review into methods, applications, and current developments. *Journal Of Magnetic Resonance Imaging*, 57(5), 1320-1339. doi:10.1002/jmri.28540





Version: Publisher's Version

License: [Creative Commons CC BY-NC-ND 4.0 license](https://creativecommons.org/licenses/by-nc-nd/4.0/)

Downloaded from: <https://hdl.handle.net/1887/3567673>

**Note:** To cite this publication please use the final published version (if applicable).

# Particle Tracing Based on 4D Flow Magnetic Resonance Imaging: A Systematic Review into Methods, Applications, and Current Developments

Paul R. Roos, MS,<sup>1\*</sup>  Friso M. Rijnberg, MD,<sup>2</sup>  Jos J. M. Westenberg, PhD,<sup>1</sup>  and Hildo J. Lamb, MD, PhD<sup>1</sup> 

**Background:** Particle tracing based on 4D Flow MRI has been applied as a quantitative and qualitative postprocessing technique to study temporally evolving blood flow patterns.

**Purpose:** To systematically review the various methods to perform 4D Flow MRI-based particle tracing, as well as the clinical value, clinical applications, and current developments of the technique.

**Study type:** The study type is systematic review.

**Subjects:** Patients with cardiovascular disease (such as Marfan, Fontan, Tetralogy of Fallot), healthy controls, and cardiovascular phantoms that received 4D Flow MRI with particle tracing.

**Field Strength/Sequence:** Three-dimensional three-directional cine phase-contrast MRI, at 1.5 T and 3 T.

**Assessment:** Two systematic searches were performed on the PubMed database using Boolean operators and the relevant key terms covering 4D Flow MRI and particle tracing. One systematic search was focused on particle tracing methods, whereas the other on applications. Additional articles from other sources were sought out and included after a similar inspection. Particle tracing methods, clinical applications, clinical value, and current developments were extracted.

**Statistical Tests:** The main results of the included studies are summarized, without additional statistical analysis.

**Results:** Of 127 unique articles retrieved from the initial search, 56 were included (28 for methods and 54 for applications). Most articles that described particle tracing methods used an adaptive timestep, a fourth order Runge–Kutta integration method, and linear interpolation in the time dimension. Particle tracing was applied in heart chambers, aorta, venae cavae, Fontan circulation, pulmonary arteries, abdominal vasculature, peripheral arteries, carotid arteries, and cerebral vasculature. Applications were grouped as intravascular, intracardiac, flow stasis, and research.

**Data Conclusions:** Particle tracing based on 4D Flow MRI gives unique insight into blood flow in several cardiovascular diseases, but the quality depends heavily on the MRI data quality. Further studies are required to evaluate the clinical value of the technique for different cardiovascular diseases.

**Evidence Level:** 5.

**Technical Efficacy:** Stage 1.

J. MAGN. RESON. IMAGING 2023;57:1320–1339.

Cardiovascular disease (CVD) is the leading cause of death worldwide, with approximately 18 million lives lost every year.<sup>1</sup> The prevalence of acquired CVD is increasing, especially in patients aged below 50 years of age.<sup>2</sup> Furthermore, congenital CVD is the most common congenital defect in newborn babies and the number of patients surviving with

congenital CVD has greatly increased, due to advances in diagnosis and in pre-peri and post-operative care, although complications can occur later in life and may only be found during long-term follow-up.<sup>3</sup>

The most important factors for improving CVD outcomes are early detection, correct diagnosis, and adequate

View this article online at [wileyonlinelibrary.com](https://onlinelibrary.wiley.com/doi/10.1002/jmri.28540). DOI: 10.1002/jmri.28540

Received Dec 30, 2021, Accepted for publication Nov 15, 2022.

\*Address reprint requests to: P.R.R., Albinusdreef 2, 2333 ZA Leiden, The Netherlands. E-mail: [p.r.roos@lumc.nl](mailto:p.r.roos@lumc.nl)

From the <sup>1</sup>Department of Radiology, Leiden University Medical Center, Leiden, The Netherlands; and <sup>2</sup>Department of Cardiothoracic Surgery, Leiden University Medical Center, Leiden, The Netherlands

This is an open access article under the terms of the [Creative Commons Attribution-NonCommercial-NoDerivs](https://creativecommons.org/licenses/by-nc-nd/4.0/) License, which permits use and distribution in any medium, provided the original work is properly cited, the use is non-commercial and no modifications or adaptations are made.

management of interventions during long-term follow-up.<sup>4</sup> It is crucial to study the development of CVD individually for each patient to choose the correct treatment, but there are not many accurate (sub)clinical markers that are useful for follow-up.<sup>4,5</sup> Blood flow patterns are among the mechanisms linked to (dys-)function of the myocardium, valves, and vessels.<sup>4</sup> Understanding these blood flow patterns and recognition of aberrant flow may contribute to improved diagnostic and prognostic accuracy for CVDs and may support early detection of subclinical disease or early recognition of complications.

Cardiovascular magnetic resonance imaging (in short: cardiac MRI) is an imaging technique that can noninvasively assess the function and structure of the cardiovascular system by generating time-resolved visualizations of the blood flow within the heart and vessels.<sup>6</sup> Cardiac MRI gives a unique insight into the cardiovascular function without the risks associated with cardiac catheterization or x-ray based imaging. Four-dimensional (4D) Flow MRI has emerged as a cardiac MRI technique that combines three-dimensional (3D) spatial cine imaging with three-directional velocity-encoding phase-contrast MRI, enabling the analysis of the temporal evolution of blood flow patterns within a 3D volume.<sup>7</sup> These 4D Flow MRI scans result in large amounts of velocity data that can be visualized with pathlines or streamlines visualization, but

also with streaklines, vector plots, (nested) isosurfaces and volume rendering as demonstrated in Fig. 1.<sup>8</sup>

Particle traces are lines that show the path virtual particles follow throughout a velocity field.<sup>8</sup> In a time-varying velocity field, these particle traces are called pathlines. Comparatively, streamlines are paths that are everywhere tangent to the velocity vectors at a specific point in time.<sup>9</sup> Streamlines are therefore paths virtual particles would take in nontime-varying velocity fields, such as a single timepoint of the 4D Flow MRI data, and they can also be calculated with particle tracing.<sup>9</sup> In cardiac MRI, these particles and their pathlines represent small volumes of blood and their path throughout the cardiovascular structure, respectively. Pathlines are especially useful in unsteady velocity fields in which the flow changes over time, such as the pulsatile human blood flow.<sup>10</sup> Streamlines indicate the direction of flow at specific moments during the cardiac cycle but do not reflect the path blood actually follows over time.<sup>9</sup> The technique of following particles is called particle tracing or tracking. Besides visualization, this technique may also be used to quantify blood flow and flow patterns.<sup>8</sup> Particle tracing may be a useful diagnostic tool to evaluate patients with CVD, but it has not yet been widely applied. While there is literature describing the clinical value of particle tracing, this is inherently limited by inaccuracies in

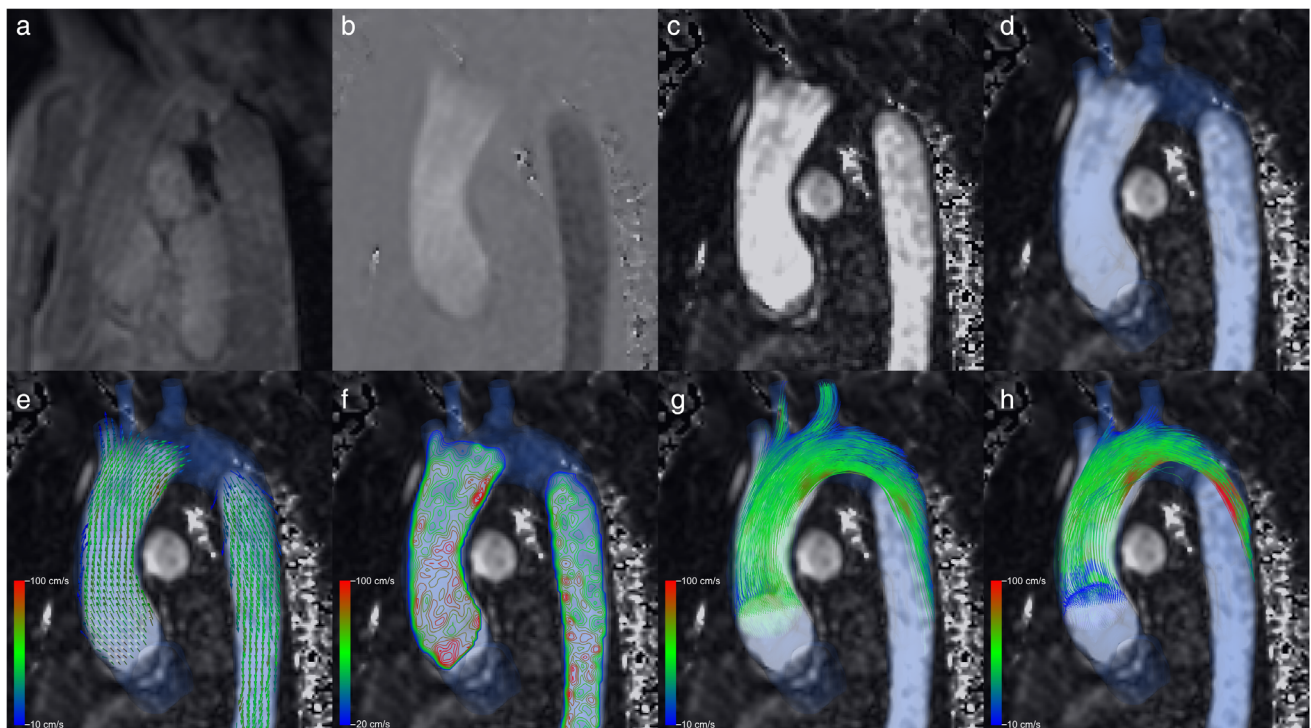


**FIGURE 1:** Example 4D Flow MRI data acquired in the thoracic aorta of a healthy volunteer with different visualization methods. (a) Magnitude image of the gradient echo. (b) Phase image of the phase-contrast data with velocity encoding in feet-head direction. (c) Magnitude image of the phase-contrast data, used for phase-contrast angiography (PCA). (d) 3D segmentation model based on PCA. (e) Vector plot displaying all velocity vectors in the image and within the segmentation model, color-coded by velocity. (f) Isoline visualization displaying areas of similar velocities. (g) Streamline visualization during peak systole, displaying the flow of virtual particles within a single timepoint in the cardiac cycle. (h) Pathline visualization, displaying the flow of virtual particles throughout the cardiac cycle. In this case, particles were released in the aortic root at early systole and traced for 300 msec.

the acquired data sets and the postprocessing technique itself.<sup>6,8,10</sup>

The present systematic review investigates current literature on the various methods applied to perform 4D Flow-based particle tracing. Furthermore, the clinical value and the clinical applications of the technique are reviewed and advice on how to perform these clinical analyses will be presented. Finally, current developments of the technique will be discussed.

## Methods

### Search Strategy and Inclusion Criteria

Two search strategies were defined, for the particle tracing methods and the applications sections respectively. For literature on 4D Flow MRI-based particle tracing methods, a search was performed in March 2022 using PubMed with following search terms: particle[Title/Abstract] AND (tracing[Title/Abstract] OR tracking[Title/Abstract] OR trace[Title/Abstract]) AND (MRI[Title/Abstract] OR magnetic resonance imaging[Title/Abstract] OR CMR[Title/Abstract]) AND (Flow[Title/Abstract] OR phase-contrast[Title/Abstract] or PC[Title/Abstract]). Retrieved publications were inspected for duplicates and vetted following the Preferred Reporting Items for Systematic Reviews and Meta-Analyses guidelines.<sup>11</sup> Stepwise filtering with the following inclusion criteria was performed by a single reviewer (PR):

1. Abstracts referencing 4D Flow MRI-based particle tracing.
2. Full texts describing particle tracing methods, for example, settings and software used, and an accuracy measurement.

For literature on 4D Flow MRI-based particle tracing applications, the following search terms were utilized in March 2022: (MRI[Title/Abstract] OR (magnetic resonance imaging[Title/Abstract]) OR CMR[Title/Abstract]) AND (Flow[Title/Abstract] OR phase-contrast[Title/Abstract] or PC[Title/Abstract]) AND ((particle tracing) OR (particle tracking)). After inspection for duplicates, retrieved literature was filtered stepwise with the following inclusion criteria by a single reviewer (P.R.):

1. Abstracts referencing 4D Flow MRI applied in the cardiovascular system.
2. Full texts include particle tracing being applied for visualization or quantification.

Current developments were identified in the discussion sections of each included article. Additional search queries were performed in Google Scholar with similar search strategies as previously mentioned, to include literature not listed in the PubMed database. Literature on non-MRI-based flow field particle tracing techniques, such as computational fluid dynamics (CFD) based particle tracing, was retrieved to

provide a summary of the technical background of particle tracing.

### Data Analysis

From the included literature, methods of particle tracing, applications of particle tracing, and the current developments of the technique were summarized. Clinically significant findings that were produced by particle tracing and delineated the clinical value of the technique were reported.

## Results

### Included Articles

A total of 54 articles (of which 1 for methods and 54 for applications) were selected from 127 unique articles after screening (Fig. 2). After exclusion of articles for particle tracing methods based on the inclusion criteria, only one article mentioned both precise particle tracing methods and an accuracy measurement. This prevents the original goal of this review to compare particle tracing methods and their outcomes. We therefore summarized the methods of 28 articles before applying the second inclusion criteria in the following sections, increasing the total number of included articles to 56 (Fig. 2). The 54 articles that were identified from the second search strategy and their main outcomes based on particle tracing are summarized in the application sections. Table 1 summarizes the included articles.

### Principles of Particle Tracing

Particle tracing was developed to visualize flow in fluid dynamics and aerodynamics.<sup>67</sup> Originally, small particles such as grain, dye or smoke were added to fluid or air flows to visualize the internal flow patterns of a larger stream. Tracking the small particles and analyzing the characteristics of their path is the basic principle of particle tracing. Nowadays, particle tracing can be done digitally in computational fluid dynamics, computational aerodynamics, or cardiovascular imaging. Other visual methods including particle imaging velocimetry have been developed.

Computational particle tracing has a simple universal basis similar to analogue particle tracing. The algorithm starts with seeding, the placement of virtual massless particles at a chosen location and time, for example, from grid-points of a rectilinear grid and releasing these particles instantly or continuously, within a four-dimensional velocity dataset.<sup>24</sup> The particles are then individually traced over time by the following three repeatable steps:

1. The velocity vector is four-dimensionally interpolated from the MRI velocity data.<sup>27,41</sup>
2. The flow velocity and direction are integrated over a specified timespan (timestep) to calculate the displacement of the particle within that time span.<sup>68</sup>

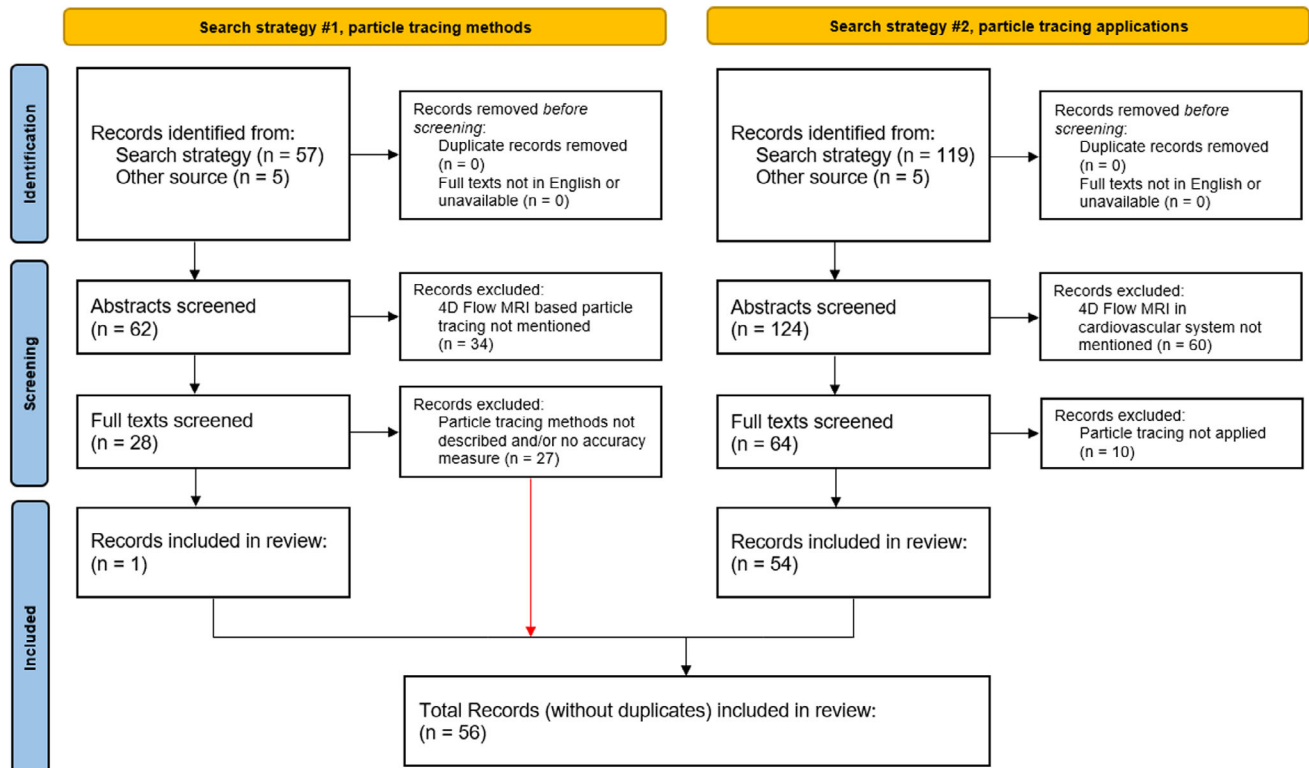


FIGURE 2: Flow diagram showing the results of the systematic search and selection process; 56 articles were included in the review after screening.

3. The new spatiotemporal (4D) location of the particle is calculated (Fig. 3). These steps are then repeated until a user-specified stopping condition is met.

As mentioned in step 3, particles are traced until a stopping condition is reached. These stopping conditions can be chosen by the user and may include a maximum particle travel distance, minimum particle velocity, leaving the structure-of-interest (3D model), maximum angle to previous trace segment, among others.

When particle tracing is complete, the particle path can be visualized as the so-called pathlines or streamlines, determined by whether the velocity data are time varying or not, respectively. Pathlines show the path of each particle over time (Fig. 3) and therefore constant or evolving flow patterns. Streamlines show the hypothetical path of each particle at a point in time and may therefore show temporary flow patterns. The pathlines can be drawn per timepoint in the 4D velocity data (timeframe) and combined in cine mode to form an animation. Color coding can be used to simplify the visual differentiation of individual particles and to add information such as particle origin, particle velocity per particle trace segment, or distance traveled (Fig. 4a–c, respectively). The number of particles traversing a structure of interest in a specific time period (i.e. flow volumes) can also be quantified and, for example, specified by categorizing the particles based on their origin or destination.<sup>24</sup>

**DISCRETE INTEGRATION.** After seeding the particles, each particle trace is calculated by integrating the velocity data. This is done using discrete integration, also called stepwise integration (Fig. 3). While the simplest discrete integration method, the Euler method, is very computationally inexpensive, it is also less accurate than more computationally expensive methods.<sup>68,69</sup> Popular methods are the Runge–Kutta methods, which are a family of higher-order methods that include the Euler method.<sup>68,70</sup> The most-used method is the fourth order Runge–Kutta method (RK4), which was applied in all 15 included articles that reported the integration method used.<sup>14,19,20,22,24,26,27,32,35,40–42,60,63,66</sup> The second-order Runge–Kutta method (RK2) might also be sufficiently accurate for particle tracing while less computationally expensive.<sup>68</sup>

This discrete integration is done over small steps in time. The length of this timestep is an important setting in particle tracing and largely defines the quality of the technique.<sup>68</sup> The optimal timestep length is predominantly dependent on the temporal resolution of the velocity data but also the spatial resolution, maximum velocity, and size of the structure of interest. The integration can also be performed using adaptive Runge–Kutta methods that change the timestep dynamically based on an error estimation, which may decrease overall computation time, but the maximum timestep should be chosen carefully to prevent quality loss.<sup>71</sup> Of the 28 articles included for particle tracing methods, only 14 specified the timestep

**TABLE 1. Summary of Included Literature on 4D Flow-Based Particle Tracing Methods and Applications**

Included reference (reference number)	Method search strategy	Applications search strategy	Software	Integrator	Timestep	Interpolation	Accuracy	Circulation
Bächler et al, 2013, Radiology <sup>12</sup>	-	Ext	-	-	-	-	-	Fontan
Bächler et al, 2013, Magn Reson Imaging <sup>13</sup>	-	Yes	-	-	-	-	-	Pulmonary
Bammer et al, 2007, Magn Reson Med <sup>14</sup>	Yes	Yes	Ensignt	RK4	Adapt	Linear time	-	Intracranial
Bastkowski et al, 2019, Radiol Cardiothorac Imaging <sup>15</sup>	-	Yes	-	-	-	-	-	Fontan
Biegging et al, 2011, J Magn Reson Imaging <sup>16</sup>	-	Yes	-	-	-	-	-	Aorta
Bolger et al, 2007, J Cardiovasc Magn Reson <sup>17</sup>	Ext	Ext	Ensignt	RK4	Adapt	Linear time	-	LV
Bunck et al, 2012, Eur J Radiol <sup>18</sup>	Ext	Yes	GTFLOW	-	-	-	Yes	Peripheral
Calkoen et al, 2014, J Thorac Imaging <sup>6</sup>	Yes	Yes	-	-	-	-	-	Intracardiac, Thoracic
Calkoen et al, 2015, Invest Radiol <sup>19</sup>	Yes	Yes	-	RK4	-	-	Yes	LV
Carlsson et al, 2011, J Cardiovasc Magn Reson <sup>20</sup>	Yes	Yes	Ensignt	RK4	Adapt	Linear time	Yes	Intracardiac
Costello et al, 2018, Int J Cardiovasc Imaging <sup>21</sup>	Yes	Yes	MATLAB	-	-	-	-	Ventricles
Dyverfeldt et al, 2011, J Magn Reson Imaging <sup>22</sup>	Yes	Yes	Ensignt	RK4	Adapt	Linear time	-	LA
Eriksson et al, 2011, Am J Physiol Heart Circ Physiol <sup>23</sup>	Ext	-	-	-	-	-	-	LV
Eriksson et al, 2010, J Cardiovasc Magn Reson <sup>24</sup>	Ext	-	-	RK4	Adapt	-	Yes	LV
Föll et al, 2013, Eur Heart J Cardiovasc Imaging <sup>25</sup>	-	Yes	-	-	-	-	-	LV

TABLE 1. Continued

Included reference (reference number)	Method search strategy	Applications search strategy	Software	Integrator	Timestep	Interpolation	Accuracy	Circulation
François et al, 2012, J Cardiovasc Magn Reson <sup>26</sup>	Yes	Yes	Ensignt	RK4	Adapt	Linear time	-	Falot (RV, PA)
Friman et al, 2011, Med Image Anal <sup>27</sup>	Yes	Yes	MeVisLab	RK4	Voxel size	Linear	-	Aorta, Carotids
Friman et al, 2010, Med Image Comput Comput Assist Interv <sup>28</sup>	-	Yes	-	-	-	-	-	Aorta
Frydrychowicz et al, 2012, Eur Radiol <sup>29</sup>	-	Yes	-	-	-	-	-	Aorta
Frydrychowicz et al, 2009, Interact Cardiovasc Thorac Surg <sup>30</sup>	-	Yes	-	-	-	-	-	Aortic Graft
Frydrychowicz et al, 2007, J Magn Reson Imaging <sup>31</sup>	-	Yes	-	-	-	-	-	Peripheral
Frydrychowicz et al, 2008, J Cardiovasc Magn Reson <sup>32</sup>	Yes	Yes	Ensignt	RK4	Adapt	Linear time	-	Aorta
Fyrenius et al, 1999, J Am Soc Echocardiogr <sup>33</sup>	-	Yes	-	-	-	-	-	LV
Fyrenius et al, 2001, Heart <sup>34</sup>	Yes	Yes	-	-	-	-	-	LA
Gaeta et al, 2018, Magn Reson Imaging <sup>35</sup>	Yes	Yes	MATLAB	RK4	5 ms	-	-	LA
Geiger et al, 2011, Eur Radiol <sup>36</sup>	-	Yes	-	-	-	-	-	Falot (PA, Aorta)
Geiger et al, 2012, J Magn Reson Imaging <sup>37</sup>	-	Yes	-	-	-	-	-	Aorta
Giese et al, 2014, J Cardiovasc Magn Reson <sup>38</sup>	Yes	Yes	GTFLOW	-	-	-	-	Thoracic
Hussein et al, 2020, 3D Print Med <sup>39</sup>	-	Yes	-	-	-	-	-	Heart valve phantom

TABLE 1. Continued

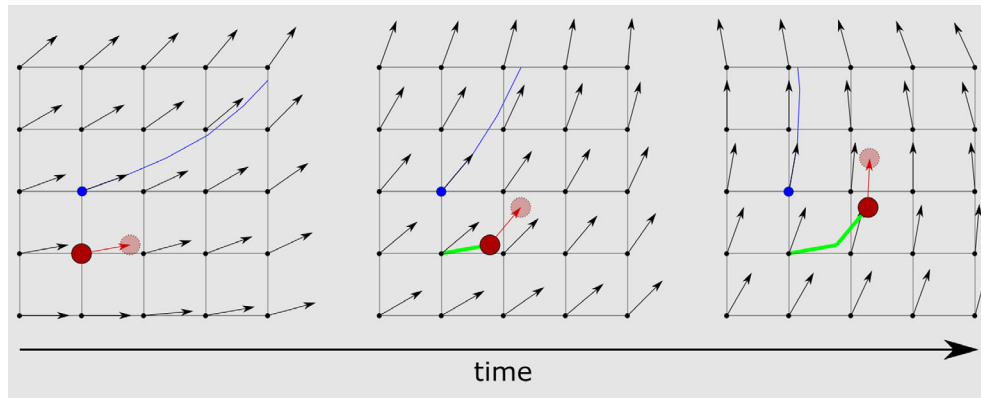
Included reference (reference number)	Method search strategy	Applications search strategy	Software	Integrator	Timestep	Interpolation	Accuracy	Circulation
Kamphuis et al, 2018, J Magn Reson Imaging <sup>40</sup>	Yes	Yes	MASS (inhouse)	RK4	8 ms	-	Yes	Intracardiac
Kanski et al, 2015, BMC Med Imaging <sup>41</sup>	Yes	Yes	-	RK4	5 ms	Linear	-	Intracardiac
Lorenz et al, 2014, Magn Reson Med <sup>42</sup>	Yes	Yes	Ensight	RK4	Adapt	Linear time	Yes	Aorta, intracranial, phantom
Markl et al, 2005, J Thorac Cardiovasc Surg <sup>43</sup>	-	Yes	-	-	-	-	-	Aorta
Markl et al, 2004, J Comput Assist Tomogr <sup>44</sup>	-	Yes	-	-	-	-	-	Aorta
Morbiducci et al, 2009, Ann Biomed Eng <sup>45</sup>	-	Yes	-	-	-	-	-	Aorta
Neuhaus et al, 2019, J Cardiovasc Magn Reson <sup>46</sup>	Yes	Yes	-	-	-	-	Yes	Aorta
Nilsson et al, 2013, Acta Radiol <sup>47</sup>	Yes	Yes	GTFLOW	-	-	-	Yes	Phantom
Reiter et al, 2013, PLoS One <sup>48</sup>	Yes	Yes	-	-	-	-	-	Pulmonary
Richter et al, 2021, Magn Reson Med <sup>49</sup>	-	Yes	-	-	-	-	-	Aorta
Rijnberg et al, 2019, Eur J Cardiothorac Surg <sup>50</sup>	-	Ext	-	-	-	-	-	Fontan
Rijnberg et al, 2021, J R Soc Interface <sup>51</sup>	-	Ext	-	-	-	-	-	Fontan
Schäfer et al, 2021, J Am Heart Assoc <sup>52</sup>	Yes	Yes	CVI42	-	-	-	-	Ventricles
Schäfer et al, 2020, J Thorac Cardiovasc Surg <sup>53</sup>	Ext	Ext	-	-	-	-	-	Fallot (LV)
Schrauben et al, 2019, J Cardiovasc Magn Reson <sup>54</sup>	-	Yes	-	-	-	-	-	Aorta, heart, fetal sheep



TABLE 1. Continued

Included reference (reference number)	Method search strategy	Applications search strategy	Software	Integrator	Timestep	Interpolation	Accuracy	Circulation
Stankovic et al, 2015, Eur Radiol <sup>55</sup>	-	Yes	-	-	-	-	-	Abdomen
Stankovic et al, 2013, Eur J Gastroenterol Hepatol <sup>56</sup>	-	Yes	-	-	-	-	-	Abdomen
Stankovic et al, 2014, Magn Reson Med <sup>57</sup>	-	Yes	-	-	-	-	-	Abdomen
Stankovic et al, 2010, J Magn Reson Imaging <sup>58</sup>	-	Yes	-	-	-	-	-	Abdomen
Stankovic et al, 2015, MAGMA <sup>59</sup>	-	Yes	-	-	-	-	-	Abdomen (liver)
Töger et al, 2011, BMC Med Imaging <sup>60</sup>	Yes	Yes	Ensignt	RK4	Adapt	Linear time	-	LV
Viola et al, 2020, J Magn Reson Imaging <sup>61</sup>	Yes	Yes	-	-	-	-	Yes	LV, Aorta
Weigang et al, 2008, Eur J Cardiothorac Surg <sup>62</sup>	-	Yes	-	-	-	-	-	Aorta
Wigström et al, 1999, Magn Reson Med <sup>63</sup>	Yes	Yes	Ensignt	RK4	Adapt	Linear time	-	Intracardiac
Wong et al, 2018, J Appl Physiol <sup>64</sup>	-	Yes	-	-	-	-	-	LV
Yamashita et al, 2007, J Magn Reson Imaging <sup>65</sup>	-	Yes	-	-	-	-	-	Intracranial
Ziegler et al, 2019, Magn Reson Imaging <sup>66</sup>	Yes	Yes	MATLAB	RK4	5 ms	-	-	Aorta

Adapt = Adaptive (timestep); Ext = External source; LA = Left atrium; LV = Left ventricle; PA = Pulmonary artery; RK4 = Fourth-order Runge–Kutta; RV = Right ventricle. Software: CVI42 (Circle Cardiovascular Imaging Inc., Calgary, Canada), Ensignt (ANSYS Inc., Canonsburg, USA), GTFlow (GyroTools LLC, Zurich, Switzerland), MATLAB (Mathworks, Natick, USA), MASS (Leiden University Medical Center, Leiden, The Netherlands), MeVisLab (MeVis Medical Solution AG, Bremen, Germany).



**FIGURE 3:** Two-dimensional illustration of tracing a virtual particle (red circle) over time in an unsteady velocity field, such as 4D Flow MRI data. The path the particle has taken is traced in green, creating a so-called pathline. In blue, a particle and its streamline is shown for each point in time.

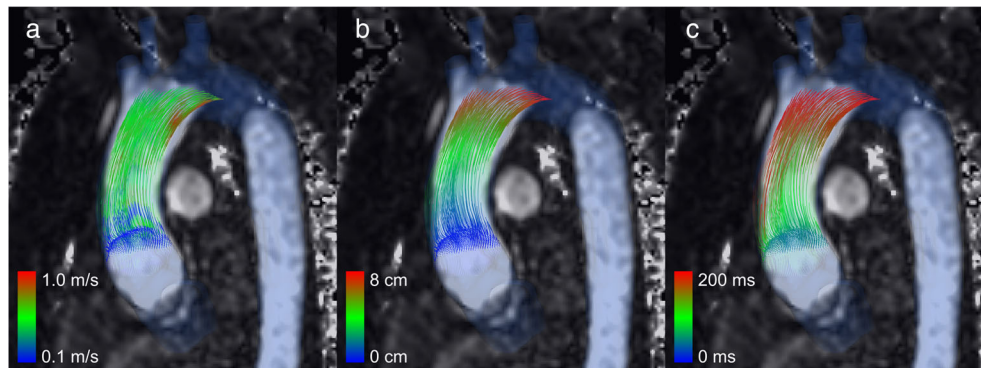


**FIGURE 4:** Pathlines with different color coding. Particles were seeded in the aortic root of a healthy volunteer at early systole and traced for 200 msec. (a) Pathlines with color coding for particle velocity (0.1–1.0 m/sec). (b) Pathlines with color coding for particle distance (0–8 cm). (c) Pathlines with color coding for particle trace time (0–200 msec). Particles outside of the segmentation (blue) were not visualized.

used. Nine of these used an adaptive Runge–Kutta method with a dynamic timestep,<sup>14,20,22,24,26,32,42,60,63</sup> while the other five used a fixed time of 5 msec,<sup>35,41,66</sup> 8 msec<sup>40</sup> or a specifically chosen size so the spatial length each step is of the same order as the grid resolution.<sup>27</sup>

**INTERPOLATION.** In the case of 4D Flow MRI data, the velocity data have the characteristics of a structured rectilinear grid, where the distance between the grid points is equal to the voxel size and the temporal resolution. The velocity data can be interpolated to find the velocity of a particle moving between the fixed grid-points. This interpolation can be done using simple computationally inexpensive methods, such as linear interpolation, or using more advanced methods such as cubic interpolation.<sup>72</sup> In all 10 included articles that reported on interpolation, it was performed using linear interpolation in the time dimension and tri-linear or tri-cubic (or other shape-function) interpolation in the space dimensions.<sup>14,20,22,26,27,32,41,42,60,63</sup> For comparison, in high-quality

CFD data, more advanced interpolation methods such as b-spline are advised.<sup>73</sup>

## ACCURACY

The settings used to perform particle tracing have an effect on how accurate and how computationally expensive the technique is. However, because only one article<sup>40</sup> reported both the exact methods of 4D Flow-based particle tracing and quantitatively assessed the accuracy, it is impossible to investigate the optimal methods based on the current literature beyond the most commonly used setting described previously. Additionally, settings advised for CFD-based particle tracing may not be suitable for 4D Flow-based particle tracing due to the differences in data quality and spatiotemporal resolution. It is therefore advised to experiment with different settings for different 4D Flow data and to always assess the accuracy, for example, by measuring the fraction of particles that wrongfully leave the cardiovascular structure through the structure wall.<sup>6</sup>

The accuracy of particle tracing is also greatly dependent on the quality of the 4D Flow data. Due to the stepwise nature of particle tracing, errors caused by noise may accumulate and result in inaccurate particle traces.<sup>27</sup> Noise may cause an inaccurate location to be calculated in the integration step, which is then used in the next integration step. It is therefore advised to perform 4D Flow MRI acquisition according to the current consensus statement to prevent artifacts and increase the signal-to-noise ratio.<sup>8</sup> Additionally, 4D Flow MRI data can be influenced by different phase offset errors such as Eddy currents, Maxwell terms, and Gradient field inhomogeneity phase offset errors. Correcting for these phase offset errors can lead to more reliable particle tracing, especially in data acquired with a low encoding velocity and higher-order background correction.<sup>42,47,61</sup>

Due to the dependency of particle tracing on the quality of the data, particle tracing outcomes can be used as a quality assessment for different 4D Flow MRI sequences<sup>20,59</sup> and postprocessing techniques,<sup>42,47,61</sup> or new applications of 4D Flow MRI, such as abdominal vasculature<sup>55,56</sup> and peripheral stents.<sup>18</sup>

In all literature included, massless particles are traced. Blood is a nonhomogeneous fluid with cells of different sizes, and massless-particle tracing is an oversimplification of the distribution of actual cells. Massed-particle tracing might be more accurate, by including more physical properties such as inertia. Unfortunately, no literature comparing massless- to massed-particle tracing in medical data could be found.

**SEEDING STRATEGIES.** The method of where and when to seed (release) the virtual particles in the velocity data determines the analysis that can be performed with particle tracing. Therefore, the desired outcomes must be determined first, and the seeding strategy should be derived from that. The precise seeding strategies for common applications are described in the respective application sections below.

Particle tracing can be performed forward in time or backward in time (by using a negative timestep in the integration or by inverting the velocity vectors of the data) to calculate their destination or origin, respectively.<sup>6,63</sup> Therefore, particles should be seeded either just before entering or just after exiting the structure of interest.<sup>6,9</sup> Alternatively, if the origin or destination of a specific volume of blood is of interest, particles can be seeded in the volume itself, for example, in each voxel, a uniform 3D grid, or with a random distribution.<sup>24,63</sup>

Seeding can be done instantaneously at one point in time, or continuously at a defined interval for a period.<sup>51,63</sup> The instantaneous method can be useful for following a specific volume of blood through the cardiovascular structure. Continuous seeding can be used to assess the entire flow over a specific time period, but this can be difficult to visualize. However, this can also be used to create streaklines, a

visualization method notably different from pathlines and streamlines.

To ensure the particles released from a 2D grid represent an equal volume of blood, Gaeta et al have developed an optimized seeding method by adjusting the time interval between releasing particles from the same location.<sup>35</sup> This may be especially useful for correct quantification of flow distributions and component analyses in atria, as described below.

## Applications

4D Flow MRI-based Particle tracing can visualize the temporal evolution of the blood flow in the acquired structure. The optimal algorithm settings, seeding strategy, and clinical value depend on the structure of interest and the MRI acquisition parameters. The resulting visualization of the flow gives insight into the efficiency of the cardiovascular structure in a way that is easy to understand and is therefore intuitive to people with various degrees of medical or technical knowledge, such as engineers, physicians, and patients.<sup>5,8</sup> Furthermore, particle tracing can be used for quantification of flow phenomena, such as flow distributions or the number and size of vortices or helices.

We included 53 articles that performed particle tracing in 4D Flow MRI of the following anatomies: heart chambers, thoracic and abdominal aorta, venae cavae, Fontan circulation, pulmonary arteries, the abdominal vasculature including the portal vein, peripheral arteries, the carotid arteries as well as the cerebral vasculature. The following sections describe each application and are grouped and preceded by the methods used.

**INTRAVASCULAR PARTICLE TRACING.** In major arteries and veins, such as the aorta, intravascular particle tracing can be applied. Commonly, a seeding grid is placed at the inlet of the cardiovascular structure of interest, for example, near the aortic root. Particles are then seeded instantaneously at the beginning of systole or diastole or continuous for a specific duration, such as an entire cardiac cycle (Fig. 5a). This is often done from seeding grids, which are placed near the proximal start of the vessel of interest. Multiple grids may be needed for complete visualization of the vessel due to the loss of particles as described above. After seeding and tracing, pathlines and streamlines can be observed for abnormal flow patterns, such as the appearance of helical or vortical flow structures (Fig. 5b,c). Alternatively, backwards intravascular particle tracing can be used to determine the origin of the blood flow. Seeding particles instantaneously or continuously can highlight a specific part of the cardiac cycle or a longer temporal interval, respectively.

In branching vessels, particle tracing can be used to quantify the distribution of flow by assessing the origins and destinations of particles. These flow distributions are

especially useful in determining flow through shunts and complex anatomies, such as the total cavopulmonary connection in Fontan patients, as explained further below.

Blood flow in major vessels may contain (almost) permanent vortices and areas with recirculating flow, aside from

the otherwise near-laminar flow. Particles seeded proximal to this vortex may follow the laminar flow around the vortex and the vortex will not be visualized or quantified by pathlines (Fig. 6a). A workaround could be localizing vessel volumes with decreased pathline density and subsequently

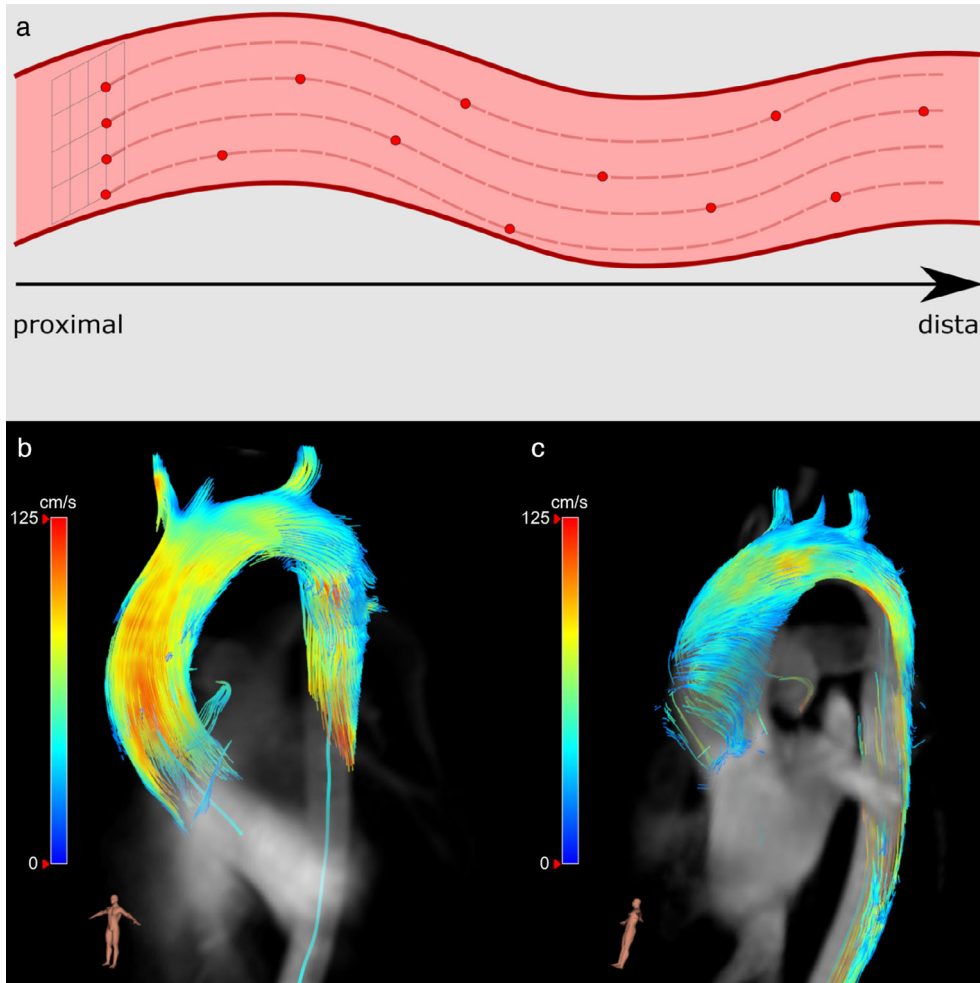


**FIGURE 5:** (a) Schematic figure of intravascular particle tracing. Virtual particles (red circles) are released from a grid inside the theoretical vessel near the origin of the blood flow and are traced as they follow the blood flow. The traced (striped) lines are the pathlines. (b) Pathlines in a healthy aorta during systole. Particles are released instantaneously from the blue planes in early systole and color coded using velocity color encoding. (c) Pathlines in an aorta with bicuspid aortic valve and aortic coarctation at the junction of the aortic arch and the descending aorta.

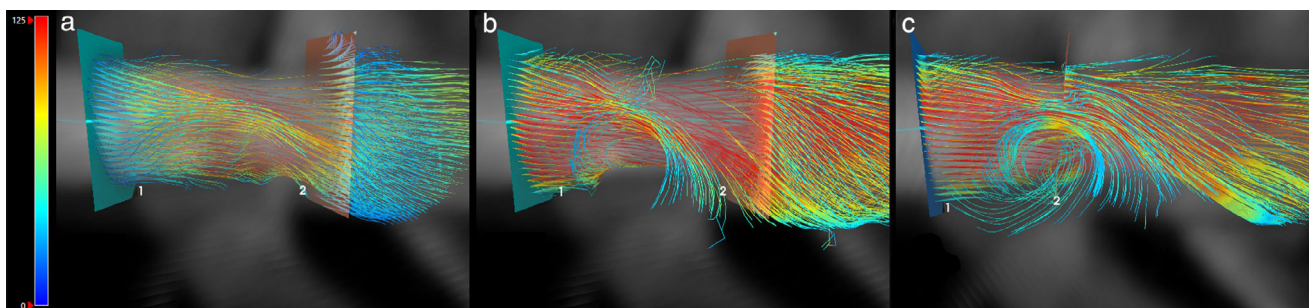


**FIGURE 6:** Vortex in descending aorta distal to coarctation as visualized with early systolic pathlines (a), late systolic streamlines (b) and late systolic pathlines (c). The vortical flow pattern is only present in late systole and diastole and may be missed by pathlines from particles seeded in early systole (a). With streamlines or pathlines from particles that are seeded in late systole (b and c, respectively), the vortex is clearly visible. By seeding particles within the vortex (c), the recirculating flow is more visible.

seeding in these less dense volumes to visualize the vortices (Fig. 6c). Alternatively, other visualization methods such as streamlines or quantification methods such as vortex quantification may be employed to find these abnormal blood flow patterns (Fig. 6b).

**AORTA.** Normal flow patterns in the thoracic aorta have been investigated with particle tracing and include right-handed helical outflow, late systolic retrograde flow, and accelerated passage through the aortic valve plane.<sup>44,45</sup> Particle tracing can distinguish between healthy volunteers and patients with thoracic aortic disease, including ascending aortic aneurysms, aortic regurgitation, and aortic dissection.<sup>44</sup> However, it is worth noting that flow patterns in the aortic arch, and maybe the entire aorta, are also related to age and ascending aorta diameter, as demonstrated with particle tracing.<sup>29</sup> To decrease acquisition times, 4D Flow MRI acquisition acceleration techniques, such as compressed-sensing or a waive-CAIPI, have been shown to be feasible in the assessment of aortic flow with particle tracing.<sup>46,49</sup>

Bicuspid aortic valve (BAV) is a congenital heart disease in which the aortic valve consists of only two cusps instead of three. This results in a decreased aortic valve aperture, an increase in blood velocity through the aortic valve, and increased wall shear stresses in the ascending aorta. It is often symptomless until adulthood and can cause other pathologies such as aortic valve stenosis (which may lead to congestive heart failure), regurgitation, and aortic aneurysm, with increased risk of aortic dissection. Using 4D Flow MRI-based particle tracing and other flow-based quantifications, helical flow patterns, increased wall shear stress and flow displacement in the ascending aorta are often present in patients with BAV.<sup>74</sup> Helical flow patterns in the ascending aorta are also related to ascending aorta dilation, which may occur with BAV.<sup>16</sup>

Aortic coarctation, a narrowing of a segment of the aorta, is a common birth defect with an overall incidence of 5%–8% of all congenital cardiac defects.<sup>75</sup> This defect typically occurs at the junction of the aortic arch and descending aorta. Coarctation is associated with other cardiovascular abnormalities including bicuspid aortic valve, arch hypoplasia, intracardiac shunts, and subaortic stenosis.<sup>76</sup> During systole, abnormal blood flow patterns such as vorticity and helicity can be observed in the aorta distal to the coarctation, which can also occur after coarctation repair and may be associated with the development of systemic hypertension.<sup>75</sup>

**FONTAN CIRCULATION.** Children with a univentricular heart defect represent the most severe end of the spectrum of congenital heart disease. The Fontan procedure is the palliative treatment of choice for these patients, in which both the superior and inferior vena cava are directly connected with the pulmonary arteries, the so-called total cavopulmonary connection (TCPC).<sup>77</sup> Therefore, the TCPC is characterized

by a cross-like shaped structure, in which opposing caval blood flow results in complex and heterogeneous blood flow patterns. Regular assessment of blood flow within this structure is important for early detection of inefficient flow patterns and flow distributions that may benefit from additional intervention (such as pulmonary artery stenting).<sup>78,79</sup>

Particle tracing provides unique insights for the cardiologist and cardiac surgeon to assess the complex blood flow, its distribution, and the possible necessity and approach of additional surgical corrections in patients with a Fontan circulation.<sup>10,80,81</sup> Abnormal blood flow can be discovered with pathlines visualization and the accompanying viscous energy loss can subsequently be quantified, as shown in inferior vena cava-Conduit mismatch.<sup>50</sup> Furthermore, particle tracing is used quantitatively to calculate the hepatic flow distribution (HFD), by determining the distribution of conduit flow, containing hepatic venous flow, toward the left and right pulmonary arteries (Fig. 7b). Hepatic venous flow contains an important “hepatic factor” that is needed in both lungs to prevent the formation of pulmonary arteriovenous malformations.<sup>12,82</sup> This quantitative measurement can only be performed with particle tracing and might identify patients at risk of pulmonary arteriovenous malformations.<sup>12</sup>

To calculate the HFD, particles are seeded continuously for the duration of one heart cycle from two seeding grids, one in the inferior vena cava and one in the superior vena cava (Fig. 7b). The particles are then traced until all have left the TCPC. Then, the fractions of the particles that have left through the left pulmonary artery, the right pulmonary artery, or through the TCPC wall (missing particles) are calculated. This type of flow distribution quantification can be applied to any bifurcating vasculature (Fig. 7a). For merging vasculature, seeding grids may be placed in the converged vessel and particles can be traced backwards to quantify the contribution of each connecting vessel.

Unfortunately, the accuracy of the HFD is limited by the spatial resolution and velocity noise. A lost particle fraction of around 20% was suggested as a cutoff condition, as the accuracy is otherwise too low to use clinically.<sup>83</sup> Unfortunately, the lost particles fraction and their effect on the clinical value of the measurement are often not reported or unknown. Figure 7b shows an example of the mixing of particles coming into the TCPC from the venae cavae and leaving through the pulmonary arteries. TCPC conduit flow is tracked as a surrogate marker of hepatic venous flow in most studies, as a uniform distribution of hepatic venous flow at the level of the conduit is often assumed, but this is not the case in most patients as shown with particle tracing.<sup>51</sup>

Flow distributions of flow originating from the venae cavae in patients with Fontan circulation and flow originating from the pulmonary trunk in healthy volunteers have been investigated using particle tracing in a 5D Flow study (4D + Respiration).<sup>15</sup> In this study, four 4D Flow datasets were

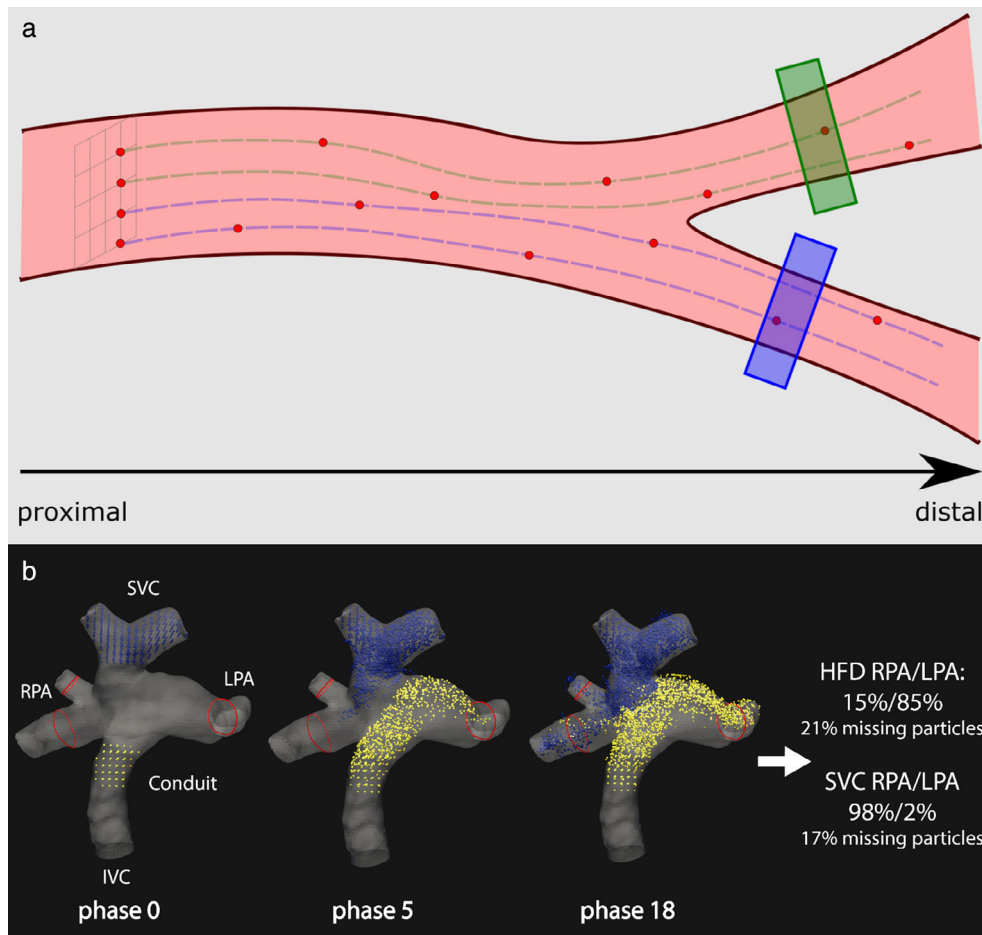


**FIGURE 7:** (a) Schematic figure of intravascular particle tracing in a bifurcating blood vessel. Virtual particles (red circles) are released from a grid inside the vessel near the origin of the blood flow and are traced as they follow the blood flow past the bifurcation. The traced (striped) lines are the pathlines, color coded with respect to their destination. Computationally, particles are labeled as blue or yellow when entering a defined area or volume (green and blue rectangles). (b) Flow distribution in a total cavopulmonary connection resulting from Fontan surgery, which connects the venae cavae directly to the pulmonary arteries in a cross-like shape. Particles are seeded continuously from three-dimensional grids in the superior (blue) and inferior (yellow) vena cava. Pathlines are not shown in this example. HFD = hepatic flow distribution, defined as IVC flow; RPA = right pulmonary artery; LPA = left pulmonary artery; SVC = superior vena cava; IVC = inferior vena cava.

reconstructed from a single acquisition, each set derived from data acquired during different part of the respiratory cycle (end-expiration, inspiration, end-inspiration, and expiration). Flow distributions to the pulmonary arteries were more respiratory dependent in patients with Fontan circulation than in healthy volunteers, especially caused by an important increase in hepatic venous flow during inspiration.<sup>15,84</sup> 4D Flow MRI acquisition may not be feasible in young patients due to long scan times and possible motion artifacts, but high acceleration factors for acquisition have been shown to have good results in Fontan patients.<sup>38</sup>

**PULMONARY CIRCULATION.** In a study by Bächler et al to determine the normal flow patterns in the pulmonary circulation, it was shown that helical flow is normally present in the main pulmonary artery (PA) and right PA.<sup>13</sup> Specifically, two counter-rotation helices were found in the main PA and in some volunteers right-handed helical flow in the right PA as

well. The helical flow was absent or substituted by abnormal vortical flow in the main PA in a patient with corrected transposition of great arteries or partial anomalous pulmonary venous return and atrial septal defect, respectively.

Pulmonary hypertension, defined as elevated mean pulmonary arterial pressure (mPAP, >25 mmHg at rest or >30 mmHg during exercise), is associated with vortical flow in the main PA.<sup>85</sup> Diagnosing pulmonary hypertension with vortex persistence based on particle tracing and pathline visualization had an area under ROC curve of 0.998, but this was similar for 3D vector, multiplanar reformatted vector and streamline visualization.<sup>48</sup> Correlation between vortex persistence and elevated mPAP was  $r = 0.92$ , meaning that particle tracing can be used for accurate diagnosis of pulmonary hypertension and estimation of elevated mPAP.<sup>48</sup>

**ABDOMINAL VASCULATURE.** In two abdominal 4D Flow feasibility studies, particle tracing was used to visualize blood

flow in a number of vessels in the splanchnic and portal arterial and venous vasculature.<sup>56,58</sup> Feasibility was judged on the visibility of the vessels in pathline visualization, which highlights the application of particle tracing for studying feasibility in new applications of 4D Flow MRI. Feasibility was shown to be good, but in a subsequent reproducibility study, a higher spatiotemporal resolution (than  $2.4 \times 2.0 \times 2.4 \text{ mm}^3$ , 61.2 msec) was recommended for complete assessment of the hepatic blood flow.<sup>57</sup> Changes in portal and splanchnic arterial hemodynamics in patients undergoing transjugular intrahepatic portosystemic shunt (TIPS) have been assessed using 4D Flow MRI.<sup>55</sup> Postoperatively increased flow rates in the portal vein, hepatic artery and in splenic and superior mesenteric arteries were identified and visualized with particle tracing.

**CAROTID ARTERIES AND INTRACRANIAL VASCULATURE.** Flow in smaller vessels, such as the intracranial arteries can be measured with 4D Flow MRI if the spatial resolution is sufficiently high enough. In an observational study to further understand the in vivo hemodynamics of the carotid arteries, particle tracing was used to assess the velocity profile and it was shown that this is parabolic (with a Womersley profile).<sup>65</sup> Furthermore, intracranial arterial flow was shown to be laminar. In another study concerning the use of acceleration techniques in cerebral 4D Flow MRI, the use of particle traces was advised to assess risk of plaque formation and progression and to assess flow dynamics and vascular patency before and after vascular interventions.<sup>14</sup>

**PERIPHERAL VASCULATURE.** Using particle tracing, Iliac and proximal femoral artery blood flow is shown to be laminar without flow accelerations or disturbances, which is in agreement with ultrasound findings.<sup>31</sup> In a patient with peripheral arterial occlusive disease, multiple flow accelerations could be identified and complex helical flow was observed distal to a moderate stenosis.<sup>31</sup> These findings are promising for the clinical value of the technique, but further studies comparing particle tracing in peripheral vasculature to standard diagnostic tools are needed.

Stents may be used in the treatment of occluding peripheral vessels but can significantly complicate MRI by stent associated artifacts. 4D Flow-based particle tracing for in-stent flow visualization has been assessed for 17 different peripheral stents and was shown to be feasible for 14 of the stents.<sup>18</sup> Particle tracing may therefore be used for assessing prestent and poststent peripheral hemodynamics.

**FLOW STASIS.** Flow stasis can occur in aneurysms and is often analyzed using contrast agents in MRI but can also be done using particle tracing by measuring the residence time of the particles.<sup>66</sup> Important limitations are the accumulation of errors during extended particle tracing, which is necessary for this type of measurement, and the low velocity-to-noise ratio

in areas with low velocities, such as areas with flow stasis. Measures such as particle travel distance analysis (TDA) and mean velocity analysis (MVA) do not rely on long particle tracing and are therefore less sensitive to measurement error, but their clinical value in aneurysms is yet to be evaluated.<sup>66</sup>

Aortic aneurysms, be it abdominal aortic aneurysms (AAAs) or thoracic aortic aneurysms (TAA), are common in the Western Countries' population and often fatal if they rupture.<sup>86</sup> Besides flow stasis analysis, particle tracing can be used to assess the blood flow patterns that occur in the aneurysm and help to identify blood flow patterns that might occur in the early stages of aneurysm development.<sup>32,62,66</sup> Especially in patients at risk for developing aortic aneurysms, such as patients with high blood pressure, high blood cholesterol, or connective tissue disorders such as Marfan syndrome and Ehlers-Danlos syndrome, 4D Flow-based particle tracing could be useful for regular check-ups and risk assessments.<sup>37,87</sup>

A study focused on hemodynamics in cerebral aneurysms revealed vortical flow patterns and velocity distributions that are determined by the aneurysm geometry, but more studies are needed to investigate a possible direct link between flow patterns and aneurysm geometries and therefore the clinical value of particle tracing for these diseases.<sup>88</sup>

The residence time of particles can be useful in anatomies other than aneurysms, such as the heart chambers. A derivative of residence time in the left and right ventricles was significantly correlated with the left and right ventricular ejection fraction, respectively.<sup>21</sup> Ventricular residence time can differentiate between patients with systolic dysfunction and healthy volunteers, but further research is still warranted.

**INTRACARDIAC PARTICLE TRACING.** "Cardiology is Flow," as flow is both the drive and result of cardiac function.<sup>4</sup> And by measuring flow, we can assess cardiac function in a direct approach instead of surrogate markers.<sup>4</sup> Myocardial dysfunction, that is, impairment of the heart muscle, can be very subtle, may progress over time, and even lead to heart failure. Lifestyle adjustments such as dietary alterations are suggested to prevent such progression.<sup>2</sup> In practice, myocardial dysfunction is defined as having a left ventricular ejection fraction of less than 40%, but flow in the heart is more complex than can be expressed by just ejection fraction. As described below, assessment of the intracardiac flow pattern may be useful in the care of patients with or at risk of cardiac disease. However, it is important to note that besides cardiac disease, some patient characteristics such as age, sex, blood pressure and heart geometry may influence intracardiac flow patterns as well.<sup>25</sup> Breathing motion compensation by respiratory gating during MRI acquisition is generally advised, but it may be feasible without.<sup>41</sup>

**MULTICOMPONENT ANALYSIS.** Wigström et al, and later improved on by Bolger et al and Eriksson et al, have

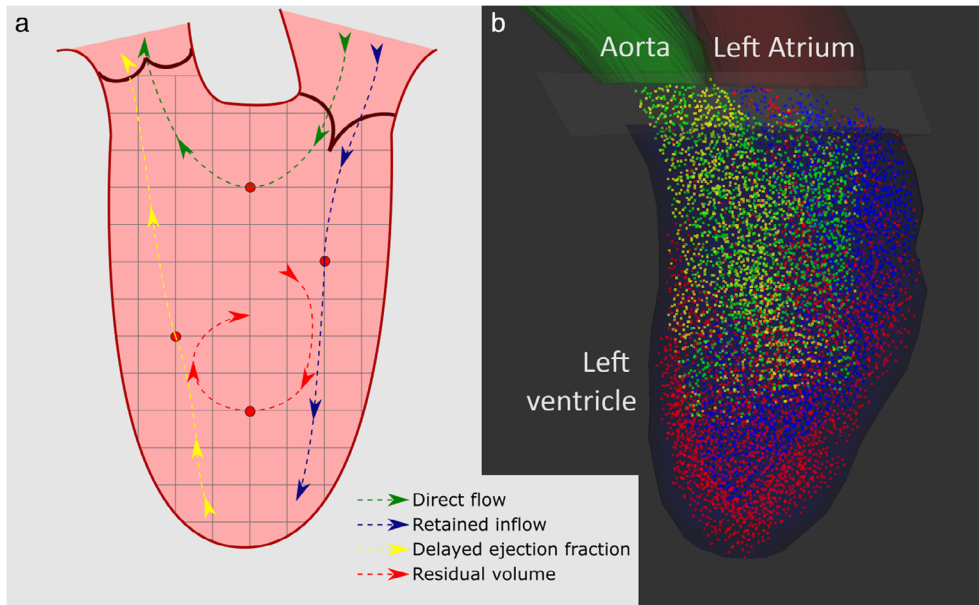


**FIGURE 8:** (a) Schematic figure of intracardiac particle tracing with four-component analysis. Virtual particles (red circles) are released from a three-dimensional grid inside the left ventricle at the end of diastole and are traced forward and backwards in time until end of systole or beginning of diastole, respectively. Particles are categorized into four components based on their origin and destination. (b) Example of particle tracing with four-component analysis in the left ventricle of a healthy volunteer just after the start of systole. A cubic model (visualized in transparent gray) was used to connect the segmentations of the left ventricle, aorta and left atrium, which were originally disconnected due to limitations of the segmentation method.

proposed a particle tracing-based four-component analysis.<sup>17,24,63</sup> For this method, particles in a heart chamber such as the left ventricle (LV) are categorized into four components based on their origin and destination within a single cardiac cycle, beginning with the diastole (Fig. 8):

1. The *direct flow* component consists of particles that enter the LV through the mitral valve and leave through the aortic valve within a single cardiac cycle.
2. The *retained inflow* component consists of particles that enter the LV through the mitral valve and remain in the LV within a single cardiac cycle.
3. The *delayed ejection flow* component consists of particles that are already in the LV and leave through the aortic valve within a single cardiac cycle.
4. The *residual volume* component consists of particles that are already in the LV and do not leave the LV within a single cardiac cycle.

The four-component analysis compares the size of these components.<sup>17</sup> It is important to note that the *delayed ejection flow* and the *retained inflow* should theoretically be equal; otherwise the volume of the LV would decrease or increase with each cardiac cycle. The ratio between *delayed ejection flow* and *retained inflow* can therefore be used as a quality control of the particle tracing algorithm.<sup>24</sup> If valvular regurgitation is expected, a regurgitation component can be added to the analysis.<sup>19</sup>

The four-component analysis requires the identification of isovolumic contraction. At this timepoint in the cardiac

cycle, at the end of diastole and the start of systole, the LV is at its largest (under normal conditions).<sup>24</sup> The LV has just started to contract, resulting in the closing of the mitral valve, and the aortic valve has not yet opened. At this time, particles are seeded in all voxels within the LV, for which a segmentation model of the epicardial contour of the LV is needed.<sup>24</sup> The particles are then traced forward in time for the duration of the systole to calculate their destination. Then, the particles are also traced backwards in time for the duration of the diastole to calculate their origin.<sup>24</sup> Virtual counter planes can be placed over the aortic and mitral valves to count particles that move through these valves. These component analyses can be used to analyze the filling and unloading of other structures, such as the other heart chambers.<sup>24</sup>

**LEFT VENTRICLE.** In a scan–rescan study of Stoll et al in 2018, it was shown that there is good reproducibility of the 4D Flow MRI-based four-component analysis in the LV, with the coefficients of variation of a similar magnitude to those of LV volumes derived from cine cardiac MRI.<sup>89</sup> This was confirmed by Kamphuis et al in a scan–rescan study in 2018, who found only small (<5%) nonsignificant mean differences for each of the four components.<sup>40</sup> In a comparison of the LV four-component analysis in patients with compensated dilated cardiomyopathy and healthy participants, Eriksson et al found a smaller direct flow fraction and altered diastolic flow routes in the patient group, besides the expected larger end-diastolic volume, smaller ejection fraction and equivalent stroke volume in the patient group.<sup>90</sup> The



flow characteristics, such as kinetic energy, can also be calculated for each component individually and may be useful markers of cardiac failure or give additional insight in cardiac disease, such as univentricular circulation.<sup>23,64</sup> When combined with more refined segmentation models such as the 16-segment LV cavity model, the distribution of components in the individual segments can be measured. This was used to quantitatively analyze the altered LV flow organization after atrioventricular septal defect correction.<sup>19</sup> Less direct flow and more retained inflow in the apical and lateral LV cavity segments were shown, and it was hypothesized that this may contribute to decreased cardiac pumping efficiency.<sup>19</sup>

**RIGHT VENTRICLE.** In a comparison of the four-component analysis of the right ventricle with the left ventricle, it was found that the direct flow fraction was larger in the right ventricle, while the residual volume was smaller.<sup>91</sup> The right ventricular direct flow fraction mostly did not extend to the apical regions but was more located at the basal regions, similar to the left ventricle. In a study that investigated the right ventricle hemodynamics after nitric oxide inhalation in children with pulmonary arterial hypertension, it was suggested that particle tracing may provide more quantitative insights into vasoreactivity testing in pulmonary hypertension than catheterization hemodynamics.<sup>52</sup>

**TETRALOGY OF FALLOT.** The venous cardiovascular system, and specifically the venae cavae and the right heart, have been investigated using intracardiac and intravascular particle tracing in patients with congenital heart defects, such as Tetralogy of Fallot (ToF), or patients with Fontan circulation (as described above). In ToF, four defects are present simultaneously, specifically a ventricular septal defect, pulmonary stenosis, over-riding aortic root, and right ventricular hypertrophy. Four-component analysis using particle tracing in patients with repaired ToF and healthy volunteers is significantly different and includes reduced direct flow and increased residual volume.<sup>26,53</sup> Furthermore, increased vortical flow patterns in the right atrium during diastole and increased helical or vortical flow features in the pulmonary arteries were shown in the patients. These vortical flow patterns in the right heart have been shown to be related to pulmonary regurgitation and may represent energy loss.<sup>92</sup> Altered flow patterns in the pulmonary arteries have been shown for different surgical techniques, indicating that particle tracing may be useful in identifying optimal surgical strategies.<sup>36</sup> Further comprehensive studies using these methods may help understand the interdependencies of geometries and hemodynamics altered post-surgically.<sup>26</sup>

**ATRIA.** While the heart ventricles are commonly assessed using the four- or five-component analysis, the atria are often analyzed using methods more similar to intravascular particle

tracing by placing seeding grids on the inlets (venae cavae for right atrium; pulmonary veins for left atrium). Visualizing the flow mixing patterns in the atria can be of interest. In the left atrium, vortical flow can be observed during systole and diastolic diastasis and inflow from the left and right pulmonary veins were shown to follow distinct paths throughout the left atrium.<sup>34</sup> These flow patterns may be beneficial in preventing left atrial stasis during normal sinus rhythm.<sup>34</sup> In mitral regurgitation, left atrial flow is notably different and related to the degree of regurgitation.<sup>22</sup>

Flow component analysis is also possible, as shown by Gaeta et al, by adjusting the seeding frequency to the velocity per grid point to ensure each particle represents the same volume of blood.<sup>35</sup> Blood entering the left atrium could subsequently be categorized into a direct flow component and a retained inflow component, similar to the intracardiac multicomponent analysis described previously. It was shown that blood entering the left atrium during systole mixes with residual blood from the previous heart cycle in a vortex.<sup>35</sup>

**RESEARCH AND NEW APPLICATIONS.** Particle tracing is often used as a quality assessment of 4D Flow MRI, for example, in new applications of 4D Flow MRI such as peripheral stents<sup>18</sup> or to compare MRI-sequences or post-processing techniques such as background phase correction.<sup>42</sup> The uncertainty of flow patterns as assessed by 4D Flow MRI can also be visualized using a probabilistic particle tracing approach, which may help interpret flow distributions and other probable flow pathways such as plaque movement.<sup>27,28</sup> New cardiovascular surgical techniques may be investigated with 4D Flow MRI-based particle tracing, as demonstrated with an anatomically shaped ascending aortic graft and other ascending aorta surgical techniques.<sup>30,43</sup> Assessment of fetal heart flow patterns with particle tracing was shown to be feasible in sheep, which may open the way to new insights and treatments of congenital heart disease.<sup>54</sup>

Both 4D Flow MRI and Doppler ultrasound aim to assess the cardiovascular system, but ultrasound has more interobserver and intraobserver variability. 4D Flow MRI-based particle tracing has been used to identify the pitfalls of Doppler evaluation of diastolic function, and may be used for Doppler ultrasound pitfalls in other cardiovascular assessments.<sup>33</sup> Additionally, particle tracing can be used to assess whether flow phantoms are comparable to human anatomy.<sup>39</sup>

## Discussion

4D Flow-based particle tracing is an effective tool to visualize time-dependent blood flows and quantify blood flow characteristics. It is intuitive to interpret and gives unique insights into complex flow patterns hitherto impossible to analyze.<sup>5,8</sup> In many cardiovascular applications, 4D Flow-based particle

tracing is already feasible and it is included in some medical software packages. However, the technique is limited by inaccuracies, the spatiotemporal resolution of the MRI data, computation time, lack of proof of clinical value and possible suboptimal settings. Particle tracing can be used in the applications shown and with the methods mentioned, but close evaluation of the accuracy and optimal settings of the technique remains advisable.

## Current Developments

**MRI ACQUISITION IMPROVEMENTS.** The clinical value of the technique is driven by its accuracy, which in turn depends heavily on the quality of the MRI data and the settings of the particle tracing technique. The accuracy may also be influenced by the use of contrast agents, and specifically blood pool agents, during acquisition. However, this only resulted in a nonsignificant visual improvement of streamlines and has not been examined with quantitative particle tracing yet.<sup>93</sup> 4D Flow MRI is a relatively new MRI technique and as such is still being improved. It is expected that these improvements will yield improvements in particle tracing as well.

A defining factor in phase contrast MRI, including 4D Flow MRI, is the encoding velocity *venc*. This user-defined factor specifies the minimum and maximum velocity that are encoded to the phase and therefore determines the range, contrast and signal-to-noise ratio (SNR) of the velocity-data. In summary, a high *venc* prevents aliasing for high velocities, but it leads to poor SNR for low velocities. A low *venc* increases the SNR for low velocities, but aliasing for high velocities. The consensus for 4D Flow MRI is to select a *venc* of 10% higher than the maximum expected velocity to avoid aliasing, but there is no consensus specifically for particle tracing.<sup>8</sup> Additionally, for many cardiovascular structures such as the heart chambers or larger (arterial) vessels, this leads to high SNR in systole, but poor SNR in diastole. New advanced phase contrast MRI sequences have been developed to incorporate multiple *venc* in the acquisition to give a good SNR for both high and low velocities. When these multi-*venc* MRI sequences become more available, the average quality and clinical value of particle tracing will be increased. Additionally, multi-*venc* approaches might lead to new applications of particle tracing that require this broad range of velocities, such as abdominal vasculature. Unfortunately, they require a decrease in temporal resolution or an increase in total acquisition time by adding additional acquisitions.<sup>94–97</sup>

The acquisition time of 4D Flow MRI can be a limiting factor in practice. This factor is often decreased by increasing the voxel size and decreasing the number of cardiac phases that are acquired. The latter, however, is often already limited by the physical acquisition speed of the scan sequence and the patient's heart rate. With more advanced k-space filling

techniques, such as artificial intelligence-driven (AI) approaches, acquisition time can be shortened. This has many advantages, such as increasing the amount of MRI exams that can be done per day. Additionally, this can increase quality by allowing for an increase in spatiotemporal resolution. Accelerated 4D Flow MRI was shown to be feasible using different acceleration factors up to  $R = 20$  times, with minimal differences.<sup>38,46,49,59,98</sup> Using acceleration methods, smaller spatiotemporal resolutions may be achieved which could theoretically improve particle tracing quality drastically, which might be shown in practice in future studies.

**POSTPROCESSING IMPROVEMENTS.** For some particle tracing methods, such as the intracardiac component particle tracing, a high-quality (4D) segmentation model of the cardiovascular structure is used for seeding and as a boundary to calculate which particles move outside of the structure during the cardiac cycle. Commonly, the endocardial contours are segmented on anatomical cine images such as short-axis or long-axis scans. They are then registered to the 4D Flow MRI scan. Other approaches include AI-based and multi-atlas approaches, which may decrease interobserver and intraobserver error.<sup>99</sup> Some of these techniques can even be used directly on the 4D Flow data, removing the necessity for additional anatomical scans, and decreasing scan times. This may lower the threshold for applying particle tracing methods that require segmentation models in the clinic.

A particle tracing timestep is advised to be shorter than the temporal resolution of the MRI data, but the 4D segmentation models have the same temporal resolution as these data. Commonly, a nearest-neighbor approach for the segmentation is used during particle tracing in between cardiac phases of the MRI data. This approach is, however, limited and can cause particles to be wrongfully regarded as outside of the segmentation when traced in between cardiac phases. A shape interpolation method more advanced than a nearest-neighbor interpolation for the segmentation, such as a simple linear or a cubic spline shape interpolation, could improve these issues.

**NEW APPLICATIONS.** We have shown an extensive summary of vasculature and cardiovascular disease that particle tracing has been applied in. In these applications, particle tracing gives unique insights into flow in the healthy, the diseased, and even the pre-clinical state. However, certainly not all CVDs that can be investigated with particle tracing have been researched thus far. Due to the nature of particle tracing, there is great potential in new applications such as post-operative assessment, thrombosis prediction, preclinical fetal studies, surgical planning, and patient specific implantation development, to name a few.<sup>18,30,36,39,54,66</sup> Research into particle tracing in these new potential applications will need to be conducted to assess the feasibility and clinical value.

## Limitations

This systematic review is limited to articles that mentioned particle tracing and 4D Flow MRI and may therefore miss information that is included in other literature. Alternative phrases such as particle tracking and 3D time-derived phase-contrast MRI were included in the search terms to include different terminology. Particle tracing can be applied in any velocity field and therefore any 4D Flow dataset, but the search terms were chosen to find literature on quantitative particle tracing results rather than just non-quantitative visualization. Other applications of particle tracing may be present in literature missed by this review due to the search terms. Nonetheless, by using two search strategies and including notable related literature, an extensive summary of particle tracing methods and applications has been put together.

## Conclusion

In summary, particle tracing based on noninvasive 4D Flow MRI provides unique insights into blood flow. Originally developed for fluid dynamics, it can visualize flow patterns in pulsatile and non-pulsatile blood flows and allows for quantification of flow distributions and flow components. With the summary of methods and applications given in this review, particle tracing can be applied accurately in blood vessels with or without bifurcations and the heart chambers. The accuracy of particle tracing depends heavily on the spatiotemporal resolution and quality of the MRI data. With the future improvements described, 4D Flow-based particle tracing may become more accurate, more versatile, and unveil more about the effect of cardiovascular diseases on blood flow. Further studies are required to evaluate the clinical value of the technique in different cardiovascular diseases.

## Acknowledgments

Additional thanks to Hans van Assen, Saša Kenjereš and Arno Roest.

## REFERENCES

- Roth GA, Mensah GA, Johnson CO, et al. Global burden of cardiovascular diseases and risk factors, 1990–2019. *J Am Coll Cardiol* 2020; 76(25):2982-3021.
- Aggarwal M, Bozkurt B, Panjath G, et al. Lifestyle modifications for preventing and treating heart failure. *J Am Coll Cardiol* 2018;72:2391-2405.
- Sun RR, Liu M, Lu L, Zheng Y, Zhang P. Congenital heart disease: Causes, diagnosis, symptoms, and treatments. *Cell Biochem Biophys* 2015; 72(3):857-860.
- Richter Y, Edelman ER. Cardiology is flow. *Circulation* 2006;113(23): 2679-2682.
- Carlhäll CJ, Bolger A. Passing strange: Flow in the failing ventricle. *Circ Heart Fail* 2010;3(2):326-331.
- Calkoen EE, Roest AAW, Van Der Geest RJ, De Roos A, Westenberg JJM. Cardiovascular function and flow by 4-dimensional magnetic resonance imaging techniques: New applications. *J Thorac Imaging* 2014;29(3):185-96.
- Stankovic Z, Allen BD, Garcia J, Jarvis KB, Markl M. 4D flow imaging with MRI. *Cardiovasc Diagn Ther* 2014;4(2):173-192.
- Dyverfeldt P, Bissell M, Barker AJ, et al. 4D flow cardiovascular magnetic resonance consensus statement. *J Cardiovasc Magn Reson* 2015; 17(1):72.
- Buonocore MH. Visualizing blood flow patterns using streamlines, arrows, and particle paths. *Magn Reson Med* 1998;40(2):210-226.
- Kamphuis VP, Westenberg JJM, van der Palen RLF, et al. Unravelling cardiovascular disease using four dimensional flow cardiovascular magnetic resonance. *Int J Cardiovasc Imaging*. 2017;33(7):1069-1081.
- Page MJ, McKenzie JE, Bossuyt PM, et al. Statement: An updated guideline for reporting systematic reviews. *BMJ* 2020;2021:n71.
- Bächler P, Valverde I, Pinochet N, et al. Caval blood flow distribution in patients with Fontan circulation: Quantification by using particle traces from 4D flow MR imaging. *Radiology* 2013;267(1):67-75.
- Bachler P, Pinochet N, Sotelo J, et al. Assessment of normal flow patterns in the pulmonary circulation by using 4D magnetic resonance velocity mapping. *Magn Reson Imaging* 2013;31(2):178-188.
- Bammer R, Hope TA, Aksoy M, Alley MT. Time-resolved 3D quantitative flow MRI of the major intracranial vessels: Initial experience and comparative evaluation at 1.5T and 3.0T in combination with parallel imaging. *Magn Reson Med* 2007;57(1):127-140.
- Bastkowski R, Bindermann R, Brockmeier K, Weiss K, Maintz D, Giese D. Respiration dependency of Caval blood flow in patients with Fontan circulation: Quantification using 5D flow MRI. *Radiology* 2019; 1(4):e190005.
- Biegling ET, Frydrychowicz A, Wentland A, et al. In vivo three-dimensional MR wall shear stress estimation in ascending aortic dilatation. *J Magn Reson Imaging* 2011;33(3):589-597.
- Bolger AF, Heiberg E, Karlsson M, et al. Transit of blood flow through the human left ventricle mapped by cardiovascular magnetic resonance. *J Cardiovasc Magn Reson* 2007;9(5):741-747.
- Bunck AC, Juttner A, Kroger JR, et al. 4D phase contrast flow imaging for in-stent flow visualization and assessment of stent patency in peripheral vascular stents—a phantom study. *Eur J Radiol* 2012;81(9): e929-e937.
- Calkoen EE, De Koning PJH, Blom NA, et al. Disturbed intracardiac flow organization after atrioventricular septal defect correction as assessed with 4D flow magnetic resonance imaging and quantitative particle tracing. *Invest Radiol* 2015;50(12):850-857.
- Carlsson M, Töger J, Kanski M, et al. Quantification and visualization of cardiovascular 4D velocity mapping accelerated with parallel imaging or k-t BLAST: Head to head comparison and validation at 1.5 T and 3 T. *J Cardiovasc Magn Reson* 2011;13(1):55.
- Costello BT, Qadri M, Price B, et al. The ventricular residence time distribution derived from 4D flow particle tracing: A novel marker of myocardial dysfunction. *Int J Cardiovasc Imaging* 2018;34(12):1927-1935.
- Dyverfeldt P, Kvitting J-PE, Carlhäll CJ, et al. Hemodynamic aspects of mitral regurgitation assessed by generalized phase-contrast MRI. *J Magn Reson Imaging* 2011;33(3):582-588.
- Eriksson J, Dyverfeldt P, Engvall J, Bolger AF, Ebberts T, Carlhäll CJ. Quantification of presystolic blood flow organization and energetics in the human left ventricle. *Am J Physiol Heart Circ Physiol* 2011;300(6): H2135-H2141.
- Eriksson J, Carlhäll C, Dyverfeldt P, Engvall J, Bolger A, Ebberts T. Semi-automatic quantification of 4D left ventricular blood flow. *J Cardiovasc Magn Reson* 2010;12(1):9.
- Föll D, Taeger S, Bode C, Jung B, Markl M. Age, gender, blood pressure, and ventricular geometry influence normal 3D blood flow characteristics in the left heart. *Eur Heart J Cardiovasc Imaging* 2013;14(4): 366-373.
- François CJ, Srinivasan S, Schiebler ML, et al. 4D cardiovascular magnetic resonance velocity mapping of alterations of right heart flow patterns and main pulmonary artery hemodynamics in tetralogy of Fallot. *J Cardiovasc Magn Reson* 2012;14(1):16.

27. Friman O, Hennemuth A, Harloff A, Bock J, Markl M, Peitgen HO. Probabilistic 4D blood flow tracking and uncertainty estimation. *Med Image Anal* 2011;15(5):720-728.
28. Friman O, Hennemuth A, Harloff A, Bock J, Markl M, Peitgen H-O. Probabilistic 4D blood flow mapping. *Medical image computing and computer-assisted intervention – MICCAI 2010*. Berlin, Heidelberg: Springer; 2010. p 416-423.
29. Frydrychowicz A, Berger A, Munoz Del Rio A, et al. Interdependencies of aortic arch secondary flow patterns, geometry, and age analysed by 4-dimensional phase contrast magnetic resonance imaging at 3 tesla. *Eur Radiol* 2012;22(5):1122-1130.
30. Frydrychowicz A, Berger A, Stalder AF, Markl M. Preliminary results by flow-sensitive magnetic resonance imaging after Tiron David I procedure with an anatomically shaped ascending aortic graft☆. *Interact Cardiovasc Thorac Surg* 2009;9(2):155-158.
31. Frydrychowicz A, Winterer JT, Zaitsev M, et al. Visualization of iliac and proximal femoral artery hemodynamics using time-resolved 3D phase contrast MRI at 3T. *J Magn Reson Imaging* 2007;25(5):1085-1092.
32. Frydrychowicz A, Arnold R, Hirtler D, et al. Multidirectional flow analysis by cardiovascular magnetic resonance in aneurysm development following repair of aortic coarctation. *J Cardiovasc Magn Reson* 2008;10(1):30.
33. Fyrenius A, Wigström L, Bolger AF, et al. Pitfalls in doppler evaluation of diastolic function: Insights from 3-dimensional magnetic resonance imaging. *J Am Soc Echocardiogr* 1999;12(10):817-826.
34. Fyrenius A, Wigström L, Ebbers T, Karlsson M, Engvall J, Bolger AF. Three dimensional flow in the human left atrium. *Heart* 2001;86(4):448-455.
35. Gaeta S, Dyverfeldt P, Eriksson J, Carlhäll CJ, Ebbers T, Bolger AF. Fixed volume particle trace emission for the analysis of left atrial blood flow using 4D flow MRI. *Magn Reson Imaging* 2018;47:83-88.
36. Geiger J, Markl M, Jung B, et al. 4D-MR flow analysis in patients after repair for tetralogy of Fallot. *Eur Radiol* 2011;21(8):1651-1657.
37. Geiger J, Markl M, Herzer L, et al. Aortic flow patterns in patients with Marfan syndrome assessed by flow-sensitive four-dimensional MRI. *J Magn Reson Imaging* 2012;35(3):594-600.
38. Giese D, Wong J, Greil GF, Buehrer M, Schaeffter T, Kozerke S. Towards highly accelerated Cartesian time-resolved 3D flow cardiovascular magnetic resonance in the clinical setting. *J Cardiovasc Magn Reson* 2014;16(1):42.
39. Hussein N, Voyer-Nguyen P, Portnoy S, et al. Simulation of semilunar valve function: Computer-aided design, 3D printing and flow assessment with MR. *3D Print Med* 2020;6(1):2.
40. Kamphuis VP, van der Palen RLF, de Koning PJH, et al. In-scan and scan-rescan assessment of LV in- and outflow volumes by 4D flow MRI versus 2D planimetry. *J Magn Reson Imaging* 2018;47(2):511-522.
41. Kanski M, Töger J, Steding-Ehrenborg K, et al. Whole-heart four-dimensional flow can be acquired with preserved quality without respiratory gating, facilitating clinical use: A head-to-head comparison. *BMC Med Imaging* 2015;15(1):20.
42. Lorenz R, Bock J, Snyder J, Korvink JG, Jung BA, Markl M. Influence of eddy current, Maxwell and gradient field corrections on 3D flow visualization of 3D CINE PC-MRI data. *Magn Reson Med* 2014;72(1):33-40.
43. Markl M, Draney MT, Miller DC, et al. Time-resolved three-dimensional magnetic resonance velocity mapping of aortic flow in healthy volunteers and patients after valve-sparing aortic root replacement. *J Thorac Cardiovasc Surg* 2005;130(2):456-463.
44. Markl M, Draney MT, Hope MD, et al. Time-resolved 3-dimensional velocity mapping in the thoracic aorta: Visualization of 3-directional blood flow patterns in healthy volunteers and patients. *J Comput Assist Tomogr* 2004;28(4):459-468.
45. Morbiducci U, Ponzini R, Rizzo G, et al. In vivo quantification of helical blood flow in human aorta by time-resolved three-dimensional cine phase contrast magnetic resonance imaging. *Ann Biomed Eng* 2009;37(3):516-531.
46. Neuhaus E, Weiss K, Bastkowski R, Koopmann J, Maintz D, Giese D. Accelerated aortic 4D flow cardiovascular magnetic resonance using compressed sensing: Applicability, validation and clinical integration. *J Cardiovasc Magn Reson* 2019;21(1):65.
47. Nilsson A, Bloch KM, Toger J, Heiberg E, Stahlberg F. Accuracy of four-dimensional phase-contrast velocity mapping for blood flow visualizations: A phantom study. *Acta Radiol* 2013;54(6):663-671.
48. Reiter U, Reiter G, Kovacs G, et al. Evaluation of elevated mean pulmonary arterial pressure based on magnetic resonance 4D velocity mapping: Comparison of visualization techniques. *PLoS ONE* 2013;8(12):e82212.
49. Richter JAJ, Wech T, Weng AM, et al. Accelerated aortic 4D flow MRI with wave-CAIPI. *Magn Reson Med* 2021;85(5):2595-2607.
50. Rijnberg F, Elbaz M, Westenberg J, et al. Four-dimensional flow magnetic resonance imaging-derived blood flow energetics of the inferior vena cava-to-extracardiac conduit junction in Fontan patients. *Eur J Cardiothorac Surg* 2019;55(6):1202-1210.
51. Rijnberg FM, Van Der Woude SFS, Van Assen HC, et al. Non-uniform mixing of hepatic venous flow and inferior vena cava flow in the Fontan conduit. *J R Soc Interface* 2021;18(177):20201027.
52. Schäfer M, Frank BS, Ivy DD, et al. Short-term effects of inhaled nitric oxide on right ventricular flow hemodynamics by 4-dimensional-flow magnetic resonance imaging in children with pulmonary arterial hypertension. *J Am Heart Assoc* 2021;10(8):e020548.
53. Schafer M, Browne LP, Jaggars J, et al. Abnormal left ventricular flow organization following repair of tetralogy of Fallot. *J Thorac Cardiovasc Surg* 2020;160(4):1008-1015.
54. Schrauben EM, Saini BS, Darby JRT, et al. Fetal hemodynamics and cardiac streaming assessed by 4D flow cardiovascular magnetic resonance in fetal sheep. *J Cardiovasc Magn Reson* 2019;21(1):8.
55. Stankovic Z, Rössle M, Euringer W, et al. Effect of TIPS placement on portal and splanchnic arterial blood flow in 4-dimensional flow MRI. *Eur Radiol* 2015;25(9):2634-2640.
56. Stankovic Z, Csatori Z, Deibert P, et al. A feasibility study to evaluate splanchnic arterial and venous hemodynamics by flow-sensitive 4D MRI compared with Doppler ultrasound in patients with cirrhosis and controls. *Eur J Gastroenterol Hepatol* 2013;25(6):669-675.
57. Stankovic Z, Jung B, Collins J, et al. Reproducibility study of four-dimensional flow MRI of arterial and portal venous liver hemodynamics: Influence of spatio-temporal resolution. *Magn Reson Med* 2014;72(2):477-484.
58. Stankovic Z, Frydrychowicz A, Csatori Z, et al. MR-based visualization and quantification of three-dimensional flow characteristics in the portal venous system. *J Magn Reson Imaging* 2010;32(2):466-475.
59. Stankovic Z, Fink J, Collins JD, et al. K-t GRAPPA-accelerated 4D flow MRI of liver hemodynamics: Influence of different acceleration factors on qualitative and quantitative assessment of blood flow. *MAGMA* 2015;28(2):149-159.
60. Töger J, Carlsson M, Söderlind G, Arheden H, Heiberg E. Volume tracking: A new method for quantitative assessment and visualization of intracardiac blood flow from three-dimensional, time-resolved, three-component magnetic resonance velocity mapping. *BMC Med Imaging* 2011;11(1):10.
61. Viola F, Dyverfeldt P, Carlhäll CJ, Ebbers T. Data quality and optimal background correction order of respiratory-gated k-space segmented spoiled gradient Echo (SGRE) and Echo planar imaging (EPI)-based 4D flow MRI. *J Magn Reson Imaging* 2020;51(3):885-896.
62. Weigang E, Kari FA, Beyersdorf F, et al. Flow-sensitive four-dimensional magnetic resonance imaging: Flow patterns in ascending aortic aneurysms. *Eur J Cardiothorac Surg* 2008;34(1):11-16.
63. Wigström L, Ebbers T, Fyrenius A, et al. Particle trace visualization of intracardiac flow using time-resolved 3D phase contrast MRI. *Magn Reson Med* 1999;41(4):793-799.
64. Wong J, Chabiniok R, Tibby SM, et al. Exploring kinetic energy as a new marker of cardiac function in the single ventricle circulation. *J Appl Physiol* 2018;125(3):889-900.

65. Yamashita S, Isoda H, Hirano M, et al. Visualization of hemodynamics in intracranial arteries using time-resolved three-dimensional phase-contrast MRI. *J Magn Reson Imaging* 2007;25(3):473-478.
66. Ziegler M, Welander M, Lantz J, et al. Visualizing and quantifying flow stasis in abdominal aortic aneurysms in men using 4D flow MRI. *Magn Reson Imaging* 2019;57:103-110.
67. Granger RA. *Fluid mechanics*. Mineola, NY: Dover Publications; 1995. p 896.
68. Darmofal DL, Haimes R. An analysis of 3D particle path integration algorithms. *J Comput Phys* 1996;123(1):182-195.
69. Pokrajac D, Lazic R. An efficient algorithm for high accuracy particle tracking in finite elements. *Adv Water Resour* 2002;25(4):353-369.
70. DeVries PL, Hasbun JE, DeVries PL. *A first course in computational physics*. 2nd ed. Sudbury, MA: Jones and Bartlett Publishers; 2011. p 433.
71. Dormand JR, Prince PJ. A family of embedded Runge-Kutta formulae. *J Comput Appl Math* 1980;6(1):19-26.
72. Lekien F, Marsden J. Tricubic interpolation in three dimensions. *Int J Numer Methods Eng* 2005;63(3):455-471.
73. Van Hinsberg MAT, Boonkamp JHMTT, Toschi F, Clercx HJH. Optimal interpolation schemes for particle tracking in turbulence. *Phys Rev E Stat Nonlinear Soft Matter Phys* 2013;87(4):043307.
74. Hope MD, Hope TA, Meadows AK, et al. Bicuspid aortic valve: Four-dimensional MR evaluation of ascending aortic systolic flow patterns. *Radiology* 2010;255(1):53-61.
75. Hope MD, Meadows AK, Hope TA, et al. Clinical evaluation of aortic coarctation with 4D flow MR imaging. *J Magn Reson Imaging* 2010;31(3):711-718.
76. Teo LLS, Cannell T, Babu-Narayan SV, Hughes M, Mohiaddin RH. Prevalence of associated cardiovascular abnormalities in 500 patients with aortic coarctation referred for cardiovascular magnetic resonance imaging to a tertiary center. *Pediatr Cardiol* 2011;32(8):1120-1127.
77. Be'eri E, Maier SE, Landzberg MJ, Chung T, Geva T. In vivo evaluation of fontan pathway flow dynamics by multidimensional phase-velocity magnetic resonance imaging. *Circulation* 1998;98(25):2873-2882.
78. Rijnberg FM, Hazekamp MG, Wentzel JJ, et al. Energetics of blood flow in cardiovascular disease: Concept and clinical implications of adverse energetics in patients with a fontan circulation. *Circulation* 2018;137(22):2393-2407.
79. Rijnberg FM, Van Assen HC, Juffermans JF, et al. Reduced scan time and superior image quality with 3D flow MRI compared to 4D flow MRI for hemodynamic evaluation of the Fontan pathway. *Sci Rep* 2021;11(1):6507.
80. Zhong L, Schrauben EM, Garcia J, et al. Intracardiac 4D flow MRI in congenital heart disease: Recommendations on behalf of the ISMRM Flow & Motion Study Group. *J Magn Reson Imaging* 2019;50(3):677-681.
81. Rijnberg FM, Van Assen HC, Hazekamp MG, Roest AAW, Westenberg JJM. Hemodynamic consequences of an undersized extracardiac conduit in an adult Fontan patient revealed by 4-dimensional flow magnetic resonance imaging. *Circ Cardiovasc Imaging* 2021;14(8):e012612.
82. Jarvis K, Schnell S, Barker AJ, et al. Evaluation of blood flow distribution asymmetry and vascular geometry in patients with Fontan circulation using 4-D flow MRI. *Pediatr Radiol* 2016;46(11):1507-1519.
83. Ha H, Kang H, Huh H, et al. Accuracy evaluation of blood flow distribution in the Fontan circulation: Effects of resolution and velocity noise. *J Vis* 2019;22(2):245-257.
84. van der Woude SFS, Rijnberg FM, Hazekamp MG, et al. The influence of respiration on blood flow in the Fontan circulation: Insights for imaging-based clinical evaluation of the total cavopulmonary connection. *Front Cardiovasc Med* 2021;8:683849.
85. Reiter G, Reiter U, Kovacs G, et al. Magnetic resonance-derived 3-dimensional blood flow patterns in the Main pulmonary artery as a marker of pulmonary hypertension and a measure of elevated mean pulmonary arterial pressure. *Circ Cardiovasc Imaging* 2008;1(1):23-30.
86. Gianfagna F, Veronesi G, Bertù L, et al. Prevalence of abdominal aortic aneurysms and its relation with cardiovascular risk stratification: Protocol of the risk of cardiovascular diseases and abdominal aortic aneurysm in Varese (RoCAV) population based study. *BMC Cardiovasc Disord* 2016;16(1):243.
87. Weinrich JM, Lenz A, Girdauskas E, Adam G, Von Kodolitsch Y, Bannas P. Current and emerging imaging techniques in patients with genetic aortic syndromes. *RöFo* 2020;192:50-58.
88. Meckel S, Stalder AF, Santini F, et al. In vivo visualization and analysis of 3-D hemodynamics in cerebral aneurysms with flow-sensitized 4-D MR imaging at 3 T. *Neuroradiology* 2008;50(6):473-484.
89. Stoll VM, Loudon M, Eriksson J, et al. Test-retest variability of left ventricular 4D flow cardiovascular magnetic resonance measurements in healthy subjects. *J Cardiovasc Magn Reson* 2018;20(1):15.
90. Eriksson J, Bolger AF, Ebberts T, Carlhäll CJ. Four-dimensional blood flow-specific markers of LV dysfunction in dilated cardiomyopathy. *Eur Heart J Cardiovasc Imaging* 2013;14(5):417-424.
91. Fredriksson AG, Zajac J, Eriksson J, et al. 4-D blood flow in the human right ventricle. *Am J Physiol* 2011;301(6):2344-2350.
92. Hirtler D, Garcia J, Barker AJ, Geiger J. Assessment of intracardiac flow and vorticity in the right heart of patients after repair of tetralogy of Fallot by flow-sensitive 4D MRI. *Eur Radiol* 2016;26(10):3598-3607.
93. Bock J, Frydrychowicz A, Stalder AF, et al. 4D phase contrast MRI at 3 T: Effect of standard and blood-pool contrast agents on SNR, PC-MRA, and blood flow visualization. *Magn Reson Med* 2010;63(2):330-338.
94. Moersdorf R, Treutlein M, Kroeger JR, et al. Precision, reproducibility and applicability of an undersampled multi-vec 4D flow MRI sequence for the assessment of cardiac hemodynamics. *Magn Reson Imaging* 2019;61:73-82.
95. Kroeger JR, Pavesio FC, Moersdorf R, et al. Velocity quantification in 44 healthy volunteers using accelerated multi-VENC 4D flow CMR. *Eur J Radiol* 2021;137:109570.
96. Ha H, Kim GB, Kweon J, et al. Multi-VENC acquisition of four-dimensional phase-contrast MRI to improve precision of velocity field measurement. *Magn Reson Med* 2016;75(5):1909-1919.
97. Callaghan FM, Kozor R, Sherrah AG, et al. Use of multi-velocity encoding 4D flow MRI to improve quantification of flow patterns in the aorta. *J Magn Reson Imaging* 2016;43(2):352-363.
98. Peper ES, Gottwald LM, Zhang Q, et al. Highly accelerated 4D flow cardiovascular magnetic resonance using a pseudo-spiral Cartesian acquisition and compressed sensing reconstruction for carotid flow and wall shear stress. *J Cardiovasc Magn Reson* 2020;22(1):1-15.
99. Bustamante M, Gupta V, Forsberg D, Carlhäll CJ, Engvall J, Ebberts T. Automated multi-atlas segmentation of cardiac 4D flow MRI. *Med Image Anal* 2018;49:128-140.